Applied Catalysis B: Environmental 221 (2018) 598–609

Contents lists available at ScienceDirect

Applied Catalysis B: Environmental

journal homepage: www.elsevier.com/locate/apcatb

Low-temperature CO oxidation over Ag/SiO_2 catalysts: Effect of OH/Ag ratio

V.V. Dutov[a], G.V. Mamontov[a], V.I. Zaikovskii[b,c], L.F. Liotta[d], O.V. Vodyankina[a,*]

[a] Tomsk State University, 36, Lenina Ave., Tomsk, Russian Federation
[b] Boreskov Institute of Catalysis, 5, Lavrentiev Ave., Novosibirsk, Russian Federation
[c] Novosibirsk State University, 2, Pirogova St., Novosibirsk, Russian Federation
[d] Institute of Nanostructured Materials (ISMN-CNR), Via Ugo La Malfa 153, Palermo, Italy

ARTICLE INFO

Keywords:
CO oxidation
Silver nanoparticles
Silica surface
OH/Ag ratio

ABSTRACT

Combined application of TPx methods, H_2-O_2 titration, UV–vis DRS, TGA-DSC-MS, TEM, XRD, N_2 adsorption at −196 °C allowed proving the OH/Ag molar ratio as the key parameter defining the catalytic properties of silica-supported silver (Ag/SiO_2) in low-temperature CO oxidation. A new insight into the formation of active species on the catalyst surface is presented. In this study, Ag/SiO_2 catalysts with Ag loading of 5 and 8 wt.% were prepared by incipient wetness impregnation method on the basis of commercial silicas preliminary calcined at 500, 700 and 900 °C. Detailed characterization of catalysts by physicochemical methods revealed that molar ratio between the concentration of surface OH groups (normalized to support mass) and silver amount in the prepared catalysts (OH/Ag ratio) affects the silver dispersion, structure of silver nanoparticles (NPs) and their catalytic properties. Only at optimal value of OH/Ag ratio the silver NPs are stated to possess both high dispersion and defective multidomain structure (that consists of several nanodomains) providing the adsorption of weakly bound oxygen species responsible for high catalytic activity in CO oxidation at low-temperature. Additionally, the co-existence of two types of active sites reacting with CO at room temperature with and without formation of adsorbed carbonate species is discussed. The first type of active sites was catalytically active in low-temperature CO oxidation with CO_2 release at room temperature (RT). The second type may retain surface carbonate species up to ~40–50 °C. The balance between these species shifts towards the first type for the active catalyst.

1. Introduction

The process of low-temperature CO oxidation has a large importance from both practical and theoretical points of view. Practical relevance is connected with air purification in devices for respiratory protection and protection of the environment from harmful emissions, neutralization of exhaust automotive gases during “cold start”, CO pollution control in the confined spaces (submarine, spacecraft, etc.), gas cleaning in CO_2 lasers and designing of CO sensors [1–4]. Theoretical importance is connected with investigation of reaction mechanisms of many oxidation processes as well as study of reactivity of active sites using CO oxidation as a model reaction [5,6]. The most active catalysts containing noble metals (Pd, Pt, Rh, Au and their alloys) supported on transition metal oxides (CeO_2, MnO_2, TiO_2, Fe_2O_3, etc.) are used for CO oxidation at ambient and ultra-low temperatures [7–11]. However, high costs of these catalysts limit their wide practical application. The silica-supported silver (Ag/SiO_2) and Ag/SiO_2 modified by transition metal oxides ($Ag/MO_x/SiO_2$) attract much attention as effective and relatively cheap catalysts for many oxidation reactions, particularly for deep oxidation of harmful air pollutants. The Ag/SiO_2 catalysts were investigated in total formaldehyde oxidation [12–15], toluene oxidation [16], low-temperature CO oxidation [17–20] and preferential CO oxidation in excess of hydrogen (PROX CO) [21–24]. The nanostructured materials on the basis of silver nanoparticles/clusters/ions supported on silica modified by transition metal oxides have a wide application as catalysts for oxidation of volatile organic compounds (VOCs) [16,25] and low-temperature CO oxidation [26], dehydrogenation and selective oxidation of alcohols [27–30], gas sensors [31], photocatalysts [32], etc.

As known, the Ag/SiO_2 catalysts are characterized by high activity and reaction stability in CO oxidation at ambient temperature [33–35]. Catalytic properties of the Ag/SiO_2 catalyst in CO oxidation strongly depend on the silver loading [36], preparation conditions [37,38], pretreatment conditions (inert or oxygen-containing atmosphere,

* Corresponding author.
E-mail address: vodyankina_o@mail.ru (O.V. Vodyankina).

http://dx.doi.org/10.1016/j.apcatb.2017.09.051
Received 13 July 2017; Received in revised form 18 September 2017; Accepted 22 September 2017
Available online 23 September 2017

temperature, etc.) [33,36,39] and surface properties of support [40,41]. Usually high activity of Ag/SiO_2 catalysts is attributed to subsurface oxygen [42], particle size [36,43] and oxidized silver species (Ag^+) [33]. Zhang et al. [36] investigated the effect of silver loading in detail. The Ag/SiO_2 catalysts with Ag loading of 2, 4, 8, 12 and 16 wt.% were prepared by incipient impregnation method and tested in CO oxidation. A volcano-shape dependence of catalytic activity on the silver loading was observed. An increase of the silver loading in the catalysts from 2 to 8 wt.% resulted in enhancement of catalytic performance. Further increase of the silver loading from 8 to 16 wt.% resulted in activity abatement. Thus, optimal silver loading was shown to be 8 wt.%. An oxidative pretreatment at 500 °C of the catalysts with 2 and 4 wt.% of silver resulted in formation of highly dispersed oxidized species. However, for the catalysts with 8, 12 and 16 wt.% of silver metallic nanoparticles with sizes of 8.2, 13.5 and 15.8 nm were observed. Moreover, an increase of temperature of oxidative pretreatment from 500 to 600–700 °C led to increasing of Ag particle size and, as a consequence, to abatement of activity. Thus, the optimal temperature of oxidative pretreatment for Ag/SiO_2 catalysts was 500 °C. The optimal temperature of reduction in the H_2 atmosphere was also studied. A reduction of Ag/SiO_2 catalysts at 200 °C resulted in formation of silver particles with optimal dispersion (4.5 nm) and the best catalytic performance in comparison with the catalysts with larger or smaller particle sizes. These data about particle size are in agreement with known literature data. For example, optimal Ag particle sizes for CO oxidation were 3–5 nm according to Yu [43], and 4.5 nm according to [37].

Different size-dependent effects are well known for metallic nanoparticles [44]. For example, the type of adsorbed oxygen species depends on the Ag particle sizes. *Kibis* et al. [45] reported that Ag particles with sizes of 5 nm and smaller stabilize the oxygen species with a binding energy of $E_b(O1s) > 530$ eV, indicating the molecular oxygen type. An increasing of particle size leads to formation of strongly charged atomic oxygen (oxide-like species) with a binding energy of $E_b(O1s) < 529$ eV. Moreover, silver particles with sizes above 5 nm were characterized by multidomain structure with high concentration of the intergrain boundaries. The authors proposed that the extended defects facilitate the adsorption of oxide-like oxygen on the silver surface. However, the nature and reaction ability of oxygen species adsorbed on the Ag/SiO_2 surface depending on the Ag particle sizes and their structure were not investigated.

Surface properties of silica seem to be one of the crucial factors defining the activity of the Ag/SiO_2 catalyst in CO oxidation. However, it was not thoroughly studied in comparison with other factors. An effect of the calcination temperature of silica support on the size of silver particles and catalytic properties of Ag/SiO_2 catalyst was shown in [40]. The Ag/SiO_2 catalysts on the basis of silica pre-calcined at 550, 700, 900 and 950 °C were investigated. On the basis of ^{1}H-NMR and XRD data the authors deduced that the interaction of silver species with the H-bonded silanol groups on the surface of non-calcined silica resulted in formation of relatively large Ag particles (13 nm) with low catalytic activity in the preferential CO oxidation, while the interaction of silver with isolated SiOH groups on the silica surface pre-calcined at 550 and 700 °C resulted in formation of smaller silver particles with improved catalytic performance. It was stated that the Ag/SiO_2-700 catalyst had the highest activity due to high dispersion of silver particles. An increase of the pre-calcination temperature to up to 900 and 950 °C resulted in reduction of both dispersion of silver particles and the catalytic activity. However, the authors put out of account the properties, reaction ability and quantity of the active sites for different catalysts. High activity of Ag/SiO_2-700 sample may be associated not only with a small size of Ag particles, but, for example, with higher reactivity of the active sites. Moreover, the sizes of Ag particles calculated from the XRD data using Scherrer's equation may significantly differ from the real sizes due to the defective structure of the Ag particles (one particle may consist of several crystal nanodomains).

Redispersing of silver particles supported on SiO_2 under oxidative/reductive pretreatments was not investigated thoroughly. Qu et al. [46] studied a behavior of silica-supported Ag particles under the redox treatments at different temperatures (oxidation at 500 °C followed by reduction at 25–500 °C), however, there were no data about the effect of hydroxyl coverage on the redispersing of silver.

Thus, in spite of numerous investigations an effect of silica surface properties (namely, concentration of OH groups) on the formation of active sites and catalytic activity of Ag/SiO_2 catalysts was not investigated systematically. It is necessary to obtain the quantitative relationship between catalytic properties of Ag/SiO_2 catalyst and properties of silica support in order to design the highly effective catalyst for CO oxidation. Relationship between temperature of calcination of support and catalytic activity of the Ag/SiO_2 catalysts proposed by Qu [40] cannot be used for this purpose, since the concentration of the surface OH groups (mmol/g) depends on the preparation condition of silica and its surface area.

In this work, for the first time, the ratio between the amount of OH groups (normalized to support mass) and silver loading in the prepared catalyst (OH/Ag ratio) was proposed as a crucial factor to achieve high activity of the Ag/SiO_2 catalyst. The purpose of the present research work is to study the influence of the OH/Ag ratio on the formation of active species and catalytic activity of the Ag/SiO_2 catalysts in CO oxidation.

2. Experimental

2.1. Catalyst preparation

Commercial mesoporous silica (Salavat catalyst plant, Russia) was used as initial material to prepare the catalyst supports. To achieve the predominantly mesoporous structure without micropores an initial silica (fraction 1–2 mm) was subjected to hydrothermal treatment (HT) in ammonia solution at 120 °C for 3 h, then dried at 120 °C for 3 h. The obtained silica was divided into three parts and calcined at 500, 700 and 900 °C for 5 h (denoted as SiO_2-500, SiO_2-700 and SiO_2-900, respectively).

The Ag/SiO_2 catalysts were prepared by incipient wetness impregnation method using silver nitrate as a precursor. Then the samples were dried at 70 °C overnight. The catalysts were treated in air flow at 500 °C for 30 min and then in 10% H_2/Ar flow at 200 °C for 30 min prior to the catalytic experiment. The nominal amount of silver in the prepared catalysts was 5 and 8 wt.%.

2.2. Catalytic activity tests

Catalytic activity of samples in CO oxidation was tested in a flow fixed-bed reactor at atmospheric pressure in temperature-programmed reaction (TPR) mode. Experiments were performed using 0.1 g of catalyst and gas mixture containing 1% CO + 1% O_2 in He (20 ml/min) and with a heating rate of 5 °C/min. Analysis of gas mixture was provided by quadrupole mass spectrometer UGA 300 (Stanford Research Systems, USA).

2.3. Catalyst characterization

The prepared catalysts were characterized by adsorption of N_2 at −196 °C, powder X-ray diffraction (XRD), UV–vis diffuse reflectance electron spectroscopy (UV–vis DRS), temperature-programmed reduction (TPR), thermogravimetric analysis − differential scanning calorimetry − mass spectrometry (TGA-DSC-MS), temperature-programmed desorption of oxygen (TPD-O_2), temperature programmed surface reaction of adsorbed carbon monoxide (TPSR-CO), transmission electron microscopy (TEM) and H_2-O_2 titration methods. Silica supports were characterized by temperature-programmed desorption of water (TPD-H_2O) and adsorption of N_2 at −196 °C.

X-ray diffraction (XRD) patterns were recorded on MiniFlex 600

(Japan, Rigaku) diffractometer with monochromatized Cu-K_α radiation (λ = 1.5418 Å) with a power setting of 40 kV and 15 mA. The XRD patterns were recorded in the range from 10° to 90° with a scan rate of 2°/min. TEM experiments were carried out using a JEM-2010 microscopes (JEOL, Japan) with an accelerating voltage of 200 kV and a lattice resolution of 0.14 nm.

TPR experiments were carried out using AutoChem HP chemisorption analyzer (Micromeritics, USA) equipped with thermal conductivity detector (TCD). The sample was oxidized in the air flow (20 ml/min) at 500 °C for 30 min prior to the TPR experiments. TPR experiments were performed in the temperature range from -50 to 700 °C at a heating rate of 10 °C/min using a 10% H_2/Ar mixture (flow rate of 20 ml/min).

The TGA-DSC-MS analysis of the Ag/SiO_2 samples was performed using simultaneous thermal analyzer STA 449 F1 Jupiter (Netzsch-Geratebau GmbH, Germany) coupled with quadrupole mass-spectrometer QMS 403 D Aeolos (Netzsch-Geratebau GmbH, Germany). The samples (~10 mg) were placed into Al_2O_3 crucible and heated from 30 to 750 °C in O_2 + N_2/Ar atmosphere with a total flow rate of 100 ml/min.

To investigate the interaction of oxygen with silver surface TPD-O_2 experiments were carried out. The chemisorption analyzer Chemisorb 2750 (Micromeritics, USA) coupled with the quadrupole mass spectrometer UGA-300 (Stanford Research Systems, USA) was used. The samples were oxidized in the air flow (20 ml/min) at 500 °C. TPD experiments were carried out in the temperature range from 25 to 900 °C at a heating rate of 10 °C/min in He flow (20 ml/min).

To investigate the interaction of CO molecule with the catalyst surface TPSR-CO experiments were carried out using Chemisorb 2750 coupled with UGA-300. The samples were oxidized in the air flow (20 ml/min) at 500 °C followed by reduction in H_2/Ar flow at 200 °C prior to the experiments. Then oxygen was adsorbed at 25 °C for 30 min (5% O_2/He, 20 ml/min). Adsorption of CO was performed at −70 °C (5% CO/He, 20 ml/min). Then sample was purged with He and heated from −70 to 500 °C with a heating rate of 10 °C/min in He flow (20 ml/min).

To investigate the surface properties of the prepared silica supports TPD-H_2O experiments were carried out using AutoChem HP chemisorption analyzer. Prepared samples were immersed in distilled water and held at room temperature (RT) for 1 h and then dried at 70 °C overnight. The samples were outgassed in vacuum (10^{-2} Torr) at 200 °C for 2 h prior to the TPD experiments in order to remove physically adsorbed water [47]. TPD experiment was carried out in the temperature range from 200 to 900 °C at a heating rate of 10 °C/min in He flow (flow rate of 20 ml/min). To prevent the condensation of water vapor all lines of the apparatus was heated up to 110 °C.

The surface area of the samples was measured by nitrogen sorption at −196 °C using TriStar II 3020 analyzer (Micromeritics, USA). All samples were outgassed (10^{-2} Torr) at 200 °C for 2 h prior to the experiments. The specific surface area was determined by applying the BET method. The pore size distribution was calculated from the desorption branch of the adsorption-desorption isotherm by the Barrett-Joyner-Halenda (BJH) method.

UV–vis DR electron spectra were recorded with an Evolution 600 spectrophotometer (Thermo Scientific, USA) using MgO as a standard sample.

Dispersion of Ag particles (fraction of Ag atoms exposed, D_{Ag}) and particle size ($d_{H2\text{-}O2}$ = 1.34/D_{Ag} for spherical crystallites of silver [48]) was calculated from H_2-O_2 titration data assuming that the monolayer of adsorbed oxygen corresponds to $O_{ads}/Ag_{surface}$ = 1/3 [49] and stoichiometry of H_2/O_{ads} = 1 [50,51]. The Ag/SiO_2 catalyst (oxidized in air at 500 °C and reduced in H_2/Ar at 200 °C) was pretreated in 5% O_2/He at 300 °C for 0.5 h followed by reduction in H_2/Ar at 300 °C for 0.5 h before the experiments. Oxygen was adsorbed at 170 °C (5% O_2/He, 30 ml/min, 0.5 h) and titration of the adsorbed oxygen was performed in a pulse mode at 170 °C by injecting of 500 µl of 10% H_2/Ar in the Ar flow (30 ml/min).

Table 1
Properties of SiO_2 supports.

Support	S_{BET}, m^2/g	V_p, cm^3/g[a]	D_{avg}, nm[b]	$[OH]_{200\text{-}900}$, µmol/g (OH/nm^2)[c]
SiO_2-500	177	0.70	15.8	1109 (3.8)
SiO_2-700	165	0.67	16.2	640 (2.3)
SiO_2-900	41	0.21	20.6	184 (2.7)

[a] Total pore volume at p/p^o = 0.99.
[b] Average pore diameter calculated as $D_{avg} = 4\ V_p/S_{BET}$.
[c] Quantity of OH groups desorbed in the temperature range from 200 to 900 °C in accordance with TPD-H_2O data and calculated by Eq. A1 and Eq. A2 (See Appendix A of Supplementary material).

Pulse chemisorption of CO was carried out using ChemiSorb2750 analyzer coupled with UGA-300. The Ag/SiO_2 catalyst was oxidized in air at 500 °C, reduced in H_2/Ar at 200 °C and then reoxidized at 25 °C in 5% O_2/He flow prior to the experiments. Then He flow (20 ml/min) was switched on and consecutive pulses of 5% CO/He mixture (500 µl) were injected at 25 °C.

3. Results and discussion

3.1. Support characterization

Table 1 shows textural properties of the obtained silica samples and values of concentration of surface OH groups after different thermal treatments. All supports have a mesoporous structure with pore width of 5–30 nm (See Fig. A1 (a and b), Appendix A of Supplementary material), therefore, the effect of pore size on the dispersion of silver nanoparticles is negligible. An increase of calcination temperature to up to 900 °C results in decreasing of the surface area and pore volume due to partial sintering of the structure under the elevated temperature. Variation of calcination temperature provides different concentration of OH groups normalized to support mass (µmol/g) or surface area of silica (OH/nm^2) according to the TPD-H_2O data (See Fig. A2, Appendix A of Supplementary material). Three regions of water desorption can be marked according to the model proposed by Zhuravlev [47]. Physically adsorbed water desorbs completely after outgassing of silica in vacuum up to 190–200 °C. The vicinal OH groups bound through the hydrogen bond can be removed at temperature 200–400 °C in vacuum with the formation of siloxane bridges. The process of desorption of isolated OH groups is characterized by slow velocity and occurs at temperature exceeding 400 °C in vacuum. A desorption of chemically bound water for calcined samples at temperatures above 200 °C in our case is connected with partial rehydroxylation of the silica surface during soaking of silica in water according to the scheme:

$$\equiv Si{-}O{-}Si\equiv + H_2O \rightarrow 2\ \equiv Si{-}OH$$

In addition, this process takes place during impregnation of silica with aqueous solution of $AgNO_3$. Reaction ability of siloxane bridges with respect to water depended on the pretreatment temperature, type of silica, and its preparation conditions.

3.2. Catalyst characterization

3.2.1. Effect of redox treatments on the silver state depending on the concentration of OH groups

To investigate the silver states on the silica surface the UV–vis DRS was used. Fig. 1 shows the electron diffuse reflectance (DR) spectra for the prepared 5Ag/SiO_2 samples (5 wt.% of silver) and the corresponding images of the samples after the cyclic TPO/TPR/TPO treatment. Surface plasmon resonance (SPR) of metallic silver particles was not observed for all Ag/SiO_2 catalysts after oxidative treatment at 500 °C in air flow, therefore, silver is oxidized into AgO_x (x < 0.5) species. Absorption band at ~250–280 nm is attributed to silver clusters $Ag_n^{\delta+}$ according to [36]. Subsequent reduction of the samples at

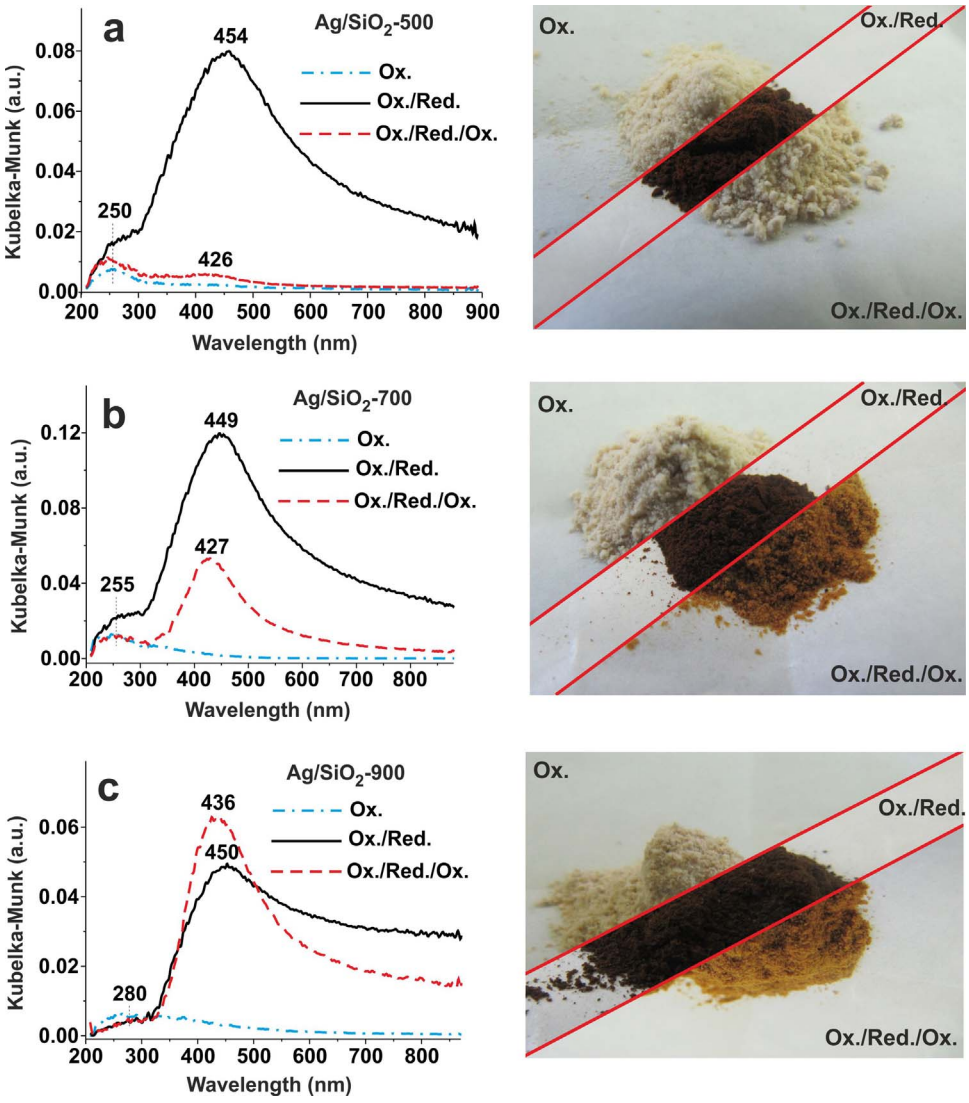

Fig. 1. UV–vis DR spectra (left) for $5Ag/SiO_2$-500 (a), $5Ag/SiO_2$-700 (b), $5Ag/SiO_2$-900 (c) samples and corresponding photographs of the samples (right) after cyclic TPO/TPR/TPO treatment.

200 °C in H_2/Ar results in appearance of the SPR (wide band with a maximum at ~450 nm) [52].

The most interesting phenomenon is observed after the second oxidative treatment at 500 °C in air. It is clearly seen that the SPR band almost disappears for the Ag/SiO_2-500 sample. According to TPR-H_2 data (See Table A1, Appendix A of Supplementary material), the quantity of the consumed hydrogen after reoxidation of Ag/SiO_2-500 sample decreases only by 7.5% in comparison with the initial oxidized state. At the same time, the band of SPR remains after the second oxidative treatment of Ag/SiO_2-700 and Ag/SiO_2-900 samples, but shifts from 450 to 427–436 nm due to decreasing of the Ag particle size [52,53]. The quantity of consumed hydrogen for the Ag/SiO_2-700 and Ag/SiO_2-900 samples after the reoxidation decreases by 36.5 and 51.6%, respectively, in comparison with the initial oxidized states. Thus, only partial redispersing and oxidation of silver particles occurs for the catalyst with low concentration of OH groups, while for the catalyst with high concentration of OH groups, both redispersing and oxidation of silver particles are almost fully reversible. Different properties and activity of silver particles supported on silica with high and low concentration of OH groups may be associated with the weakening of metal–support interaction caused by a decreasing of the concentration of OH groups. This hypothesis was confirmed by detailed investigation of Ag/SiO_2 samples.

3.2.2. *Effect of OH groups on the dispersion of AgO_x species*

The XRD patterns for oxidized $5Ag/SiO_2$ samples are presented in Fig. A3 (a), Appendix A of Supplementary material. Intensity of diffraction peak at $2\theta \sim 33^\circ$ attributed to silver oxide phase increases for Ag/SiO_2-700 and Ag/SiO_2-900 in comparison with the Ag/SiO_2-500 sample. According to calculations by Scherrer's equation, the average sizes of silver oxide particles for Ag/SiO_2-700 and Ag/SiO_2-900 are equal to 7.0 and 11.3 nm, respectively. Particle sizes for Ag/SiO_2-500 sample are close to detection limit of the XRD (about 3 nm).

To study the properties of the AgO_x species formed after the oxidative pretreatment of the catalysts TPD-O_2 experiments were carried out. Fig. 2 shows the mass spectra of O_2 evolution for Ag/SiO_2 catalysts after the oxidative pretreatment at 500 °C and bulky Ag_2O used as a reference. Two high temperature desorption peaks with a maximum at ~660–700 °C and ~760–780 °C, respectively, and one low temperature peak at 580–600 °C are observed for the Ag/SiO_2 samples. The value of ΔG_r for reaction «$2Ag + 1/2O_2 = Ag_2O$» for small Ag particles is lower (more negative) than for large particles and bulky silver in accordance with thermodynamic calculation [54]. In other words, the existence of small and highly dispersed Ag_2O particles is more beneficial then bulky Ag_2O. Indeed, bulky Ag_2O with mean crystallite sizes of 39 nm (according to XRD) decomposes at 390 °C, while the dispersed AgO_x species on the surface of silica decompose at temperatures above 600 °C according to our TPD-O_2 data. Taking into account the thermodynamic calculations [54] and XRD data, we concluded that the low

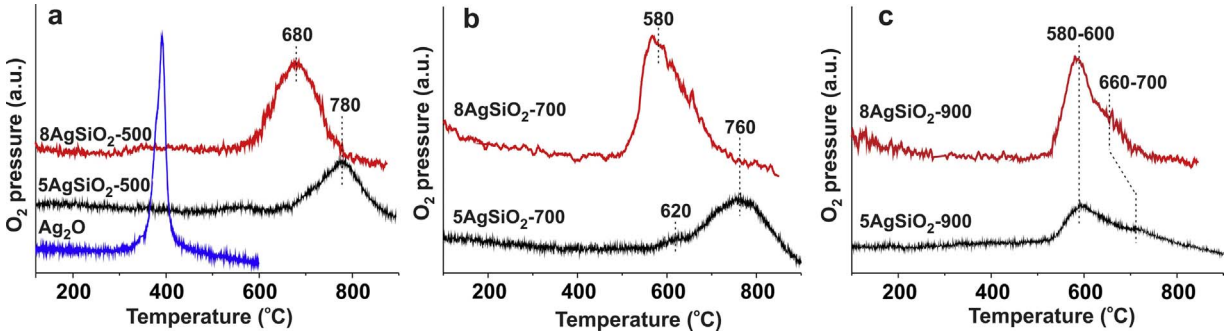

Fig. 2. TPD-O_2 profiles for Ag/SiO_2-500 (a), Ag/SiO_2-700 (b) and Ag/SiO_2-900 (c) catalysts, containing 5 and 8 wt.% of silver after oxidative pretreatment at 500 °C and bulky Ag_2O.

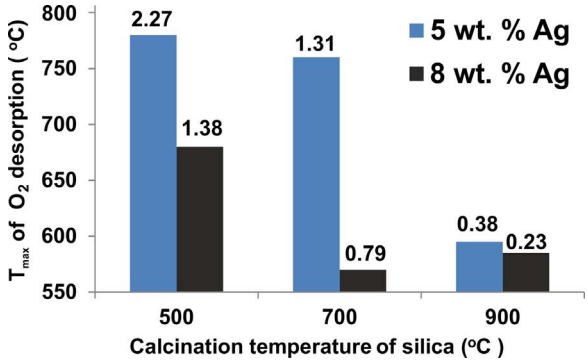

Fig. 3. Interrelation between OH/Ag ratio (above columns), calcination temperature of silica and maximum temperature of oxygen desorption for Ag/SiO_2 catalysts, containing 5 and 8 wt.% of silver.

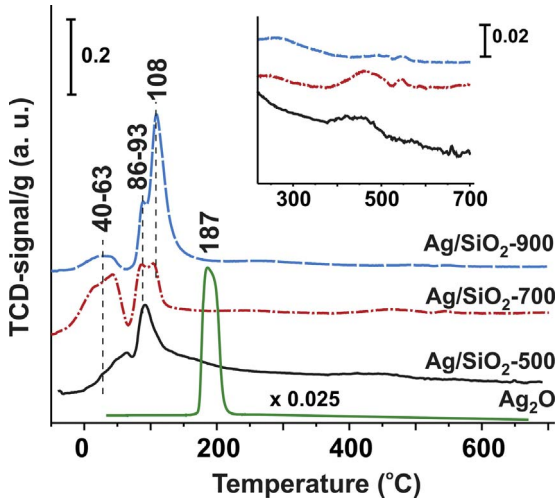

Fig. 4. TPR-H_2 profiles for 5Ag/SiO_2-500, 5Ag/SiO_2-700, 5Ag/SiO_2-900 catalysts and bulky silver oxide.

temperature desorption peak for Ag/SiO_2 samples may be associated with decomposing of relatively large Ag_2O particles (~10 nm or more), and the high temperature desorption peaks may be attributed to decomposing of the highly dispersed AgO_x species (< 3 nm), particularly, clusters of silver oxide.

Fig. 3 shows the relationship between calcination temperature of silica and oxygen desorption temperature for Ag/SiO_2 catalysts containing 5 and 8 wt.% of silver. One can see that the increase of the pre-calcination temperature of support as well as increase of silver loading in the catalysts lead to diminishing of oxygen desorption temperature caused by weakening of metal–support interaction and increase of sizes of AgO_x particles. It was previously reported that the desorption temperature of oxygen for Ag/SiO_2 catalysts is associated with a degree of metal–support interaction [55]. Taking into account the TPD-O_2 data, the molar ratio between the amounts of OH groups (normalized to support mass) and silver amount in the prepared catalyst (OH/Ag ratio) was considered as a crucial feature of Ag/SiO_2 catalysts. Thus, the TPD-O_2 and XRD data confirm the hypothesis about formation of relatively large Ag_2O particles caused by weakening of metal–support interaction for supports with low concentration of OH groups.

Fig. 4 shows the H_2-TPR profiles for 5Ag/SiO_2 catalysts after the oxidative pretreatment at 500 °C and bulky Ag_2O used as a reference sample. TPR-H_2 data are reported in Table A1, Appendix A of Supplementary material. Two regions of hydrogen consumption are observed for Ag/SiO_2 catalysts. Low-temperature region (from −50 to 200 °C) contains three intensive peaks, which may be associated with reduction of different oxidized species: type I (T_{max} = 40–63 °C), type II (T_{max} = 86–93 °C) and type III (T_{max} = 108 °C). High temperature region (from 350 to 600 °C) contains a broad peak with low intensity at ~370–460 °C, which may be associated with reduction of silver species strongly interacting with the silica support surface (namely Si-O-Ag) [56]. The amount of these species is small due to relatively low negative charge of silica surface at pH ~7. Only one peak of hydrogen consumption at 187 °C was observed for bulky silver oxide. Species of types I and II may be attributed to highly dispersed AgO_x species (x < 0.5 in accordance with TPR), particularly, clusters of silver oxide. Amount of Ag_2O species grows with increasing of the silica support calcination temperature according to the XRD data, therefore, species of type III may be attributed to Ag_2O particles.

The 5Ag/SiO_2-500 and 5Ag/SiO_2-900 samples were investigated by the TGA-DSC-MS after the impregnation procedure. The obtained results are shown in Fig. A4 (a and b), Appendix A of Supplementary material. It is clearly seen that the decomposition of supported $AgNO_3$ for the Ag/SiO_2-500 sample occurs via one step in the temperature range of 180–420 °C and is accompanied by the exothermic effect. At the same time, the decomposition of the supported $AgNO_3$ for Ag/SiO_2-900 sample is a two-step process. The first stage of the mass loss in the range of 180–350 °C is accompanied by exothermic effect, while the endothermic effect was observed for the second stage of mass loss at 360–480 °C. Appearance of two distinct thermal effects accompanying the decomposition of the $AgNO_3$ may be associated with different states of supported precursor. Decomposition of crystalline $AgNO_3$ is an endothermic process according to the thermodynamic calculations (ΔH°_{298} = 157.5 kJ/mol), therefore exothermic effect may be associated with the decomposition of amorphous $AgNO_3$, and endothermic effect attributed to crystalline $AgNO_3$. Formation of two different states of $AgNO_3$ on the surface of Ag/SiO_2-500 and Ag/$SiO_2$900 samples may be explained as follows. In the course of the impregnation procedure in aqueous solution silver ions adsorb on the negatively charged surface of SiO_2 (the isoelectric point for different silica ranged from 1 to 3 [57]) according to the scheme:

$Si{-}OH \rightarrow Si{-}O^{-} + H^{+}$ (ionization of silanol groups),

$Si{-}O^{-} + Ag^{+} \rightarrow Si{-}O{-}Ag$ (adsorption of silver ions).

The Si-O-Ag species act as nucleuses for deposition of $AgNO_3$ on the surface of silica. High concentration of the surface OH groups provides the formation of high amount of nucleuses, and, thus, the amorphous layer of $AgNO_3$ is precipitated on the SiO_2-500 support. At low concentration of the OH groups for SiO_2-900 support a homogeneous crystallization of $AgNO_3$ in the solution followed by deposition of salt crystallites on the surface occurs. Subsequent decomposition of the supported $AgNO_3$ in the oxidative atmosphere results in formation of AgO_x species with different dispersion and strength of interaction with silica surface.

To summarize, the first oxidative pretreatment of the $5Ag/SiO_2$ catalysts at 500 °C (decomposition of $AgNO_3$ accompanied by oxidation of silver particles) leads to formation of oxidized silver species with different dispersion. The highly dispersed AgO_x species are observed for $5Ag/SiO_2$-500 sample, while for the $5Ag/SiO_2$-700 and $5Ag/SiO_2$-900 samples the formation of relatively large Ag_2O particles also occurs. Silanol groups of silica are able to stabilize highly dispersed AgO_x species and prevent their aggregating. When the concentration of silanol group decreases, highly dispersed AgO_x species agglomerate with formation of relatively large oxide particles. The similar tendency takes place when silver loading in the catalyst increases, since higher amount of silver ions are shared over single OH group. Thus, the molar ratio between amounts of OH groups (normalized to support mass) and silver loading in the prepared catalyst (OH/Ag ratio) can be considered the key parameter characterizing the Ag/SiO_2 catalysts.

3.2.3. Effect of OH groups on the dispersion of silver nanoparticles

The H_2 pretreatment at 200 °C of oxidized samples results in the formation of metallic silver NPs according to the XRD (See Fig. A3(b), Appendix A of Supplementary material). Dispersion of silver particles was calculated for all samples using the H_2-O_2 titration method and TEM. Fig. 5 shows the TEM images and corresponding particle size distributions for the $5Ag/SiO_2$-500, $5Ag/SiO_2$-700 and $5Ag/SiO_2$-900 samples. It is clearly seen that the particle size distribution for the Ag/SiO_2-500 catalyst is uniform, and a predominant part of Ag NPs has sizes of 1–3 nm. However, the particle size distribution for the $5Ag/SiO_2$-700 and $5Ag/SiO_2$-900 catalyst is not uniform. Silver particles with sizes of 3–6 nm as well as those with sizes of 1–3 nm are observed for $5Ag/SiO_2$-700 and $5Ag/SiO_2$-900 catalysts. Moreover, silver particles with sizes above 10 nm are observed for $5Ag/SiO_2$-900 catalyst. Broadening of the particle size distribution leads to increase of the average particle sizes for the supports with low concentration of OH-groups. The fact of the matter is that reduction of highly dispersed AgO_x species leads to the formation of small Ag NPs with sizes of 1–3 nm, while the reduction of large Ag_2O particles produces the silver particles with the larger sizes. An increase of Ag particle sizes for $8Ag/SiO_2$ catalysts in comparison with those of $5Ag/SiO_2$ was also observed. In general, a dispersion of Ag particles depends on the OH/Ag ratio. Fig. 6 shows the correlation between the silver dispersion and OH/Ag ratio for the prepared catalysts. One can see that the dispersion of silver measured by H_2-O_2 titration method decreases with reduction of OH/Ag ratio. Fig. 7 shows the TEM images and relevant Fourier patterns for the $5Ag/SiO_2$-500 and $5Ag/SiO_2$-900 catalysts. Fourier pattern for the $5Ag/SiO_2$-900 are presented by circle reflexes corresponding to the interplanar distances of metallic silver (d_{111} = 0.23 nm), while point reflexes from planes (111) are observed for the $5Ag/SiO_2$-500 sample. Thus, silver NPs on the surface of $5Ag/SiO_2$-900 catalyst consist of several crystal domains. Earlier we reported about the formation of silver NPs with domain structure for the Ag/SiO_2-900 catalyst prepared on basis of sol-gel silica [58].

To summarize, the concentration of OH groups on the silica surface (or OH/Ag ratio) affects both the dispersion of Ag nanoparticles and their structure. Reduction of large AgO_x particles leads to formation of larger silver particles consisting of several crystal nanodomains. Formation of domain structure for large Ag NPs is connected with the higher probability of simultaneous formation of several metallic silver nucleuses during the reduction in H_2/Ar.

3.2.4. Catalytic activity of Ag/SiO_2 catalysts in CO oxidation

Fig. 8 shows the dependencies of CO conversion on the reaction temperature for the Ag/SiO_2 catalysts (5 and 8 wt.% Ag) subjected to oxidative pretreatment at 500 °C followed by reduction at 200 °C. According to the catalytic data, the activity of $5Ag/SiO_2$-700 catalyst is higher than the one for the $5Ag/SiO_2$-500. However, the activity of $5Ag/SiO_2$-900 is lower in comparison with those for $5Ag/SiO_2$-700 and $5Ag/SiO_2$-500 samples at temperature range of 45–130 °C. Values of T_{98} are equal to 105, 58 and 128 °C for $5Ag/SiO_2$-500, $5Ag/SiO_2$-700 and $5Ag/SiO_2$-900 catalysts, respectively. Decreasing of the catalytic activity for $5Ag/SiO_2$-900 in comparison with the $5Ag/SiO_2$-700 sample is associated with sintering of the SiO_2-900 support and low dispersion of silver particles, and, hence, the lowest amount of active sites that it was shown in Section 3.2.3.

From Fig. 8(b) one can see that the activities of $8Ag/SiO_2$-500 and $8Ag/SiO_2$-700 catalysts are similar. Decreasing of catalytic activity for $8Ag/SiO_2$-900 in comparison with other two samples may be associated with low dispersion of silver, as in the case of $5Ag/SiO_2$-900 catalyst. It is noteworthy that the activity of catalysts prepared on the basis of SiO_2-500 support grows up with an increase of silver loading. Values of T_{98} are equal to 66 and 105 °C for $8Ag/SiO_2$-500 and $5Ag/SiO_2$-500 catalysts, respectively. However, for SiO_2-700 support an opposite effect was observed. Values of T_{98} are equal to 73 and 58 °C for $8Ag/SiO_2$-700 and $5Ag/SiO_2$-700 catalysts, respectively. Catalytic activity of $5Ag/SiO_2$-900 and $8Ag/SiO_2$-900 catalysts was similar. Thus, the optimal loading of silver in the catalysts depends on the concentration of OH groups on the silica surface. It is noteworthy that the conversion curves for the $5Ag/SiO_2$-700, $5Ag/SiO_2$-900, $8Ag/SiO_2$-500 and $8Ag/SiO_2$-700 catalysts are characterized by double-peak activity. Conversion of CO grows with an increasing of temperature in the range from −50 °C to RT, however, after that a reduction of CO conversion (deactivation) is observed. Starting from ~35 °C conversion increases again.

Some of Ag/SiO_2 catalysts were tested in operation conditions close to those typical for air purification devices (~115 ppm CO in atmospheric air, T = 29 °C, flow rate of 100 ml/min, catalyst volume 0.5 cm^3). The data is presented in Fig. A5, Appendix A of Supplementary material. The Ag/SiO_2 catalysts demonstrate high activity (CO conversion ≥80%) and stability during 20 h on-stream.

Table 2 shows the comparison of the most active Ag/SiO_2 catalysts prepared in this work and the catalysts described in the literature sources for the last 5 years. One can see that the activity of the prepared Ag/SiO_2 catalysts in terms of T_{98} and TOF is higher or close to those for the catalysts presented in the literature. On the other side, a specific catalytic activity for our samples is higher due to relatively low surface area. Moreover, we used higher GHSV and lower concentration of oxygen in the reaction mixture.

To explain the double-peak activity and different catalytic properties of the Ag/SiO_2 samples additional experiments with pulse CO chemisorption were carried out. Fig. 9 shows the evolution of CO_2, O_2 and CO concentrations in course of CO pulse adsorption at RT on the $5Ag/SiO_2$-500 and $5Ag/SiO_2$-700 catalysts subjected to oxidative pretreatment at 500 °C followed by reduction at 200 °C and re-adsorption of oxygen at 25 °C. One can see that the first impulse of CO (marked with arrow) is almost completely absorbed without CO_2 emission into the gas phase, while the second and the subsequent impulses are partially absorbed and accompanied by CO_2 releasing. This means that some active sites on the surface of both catalysts are able to oxidize CO with formation of adsorbed carbonate species which are stable at RT. Another part of active sites also reacts with CO at RT, however, CO_2 release occurs immediately. In other words, two types of active sites exist on the surface of all Ag/SiO_2 catalysts, however, only one of them

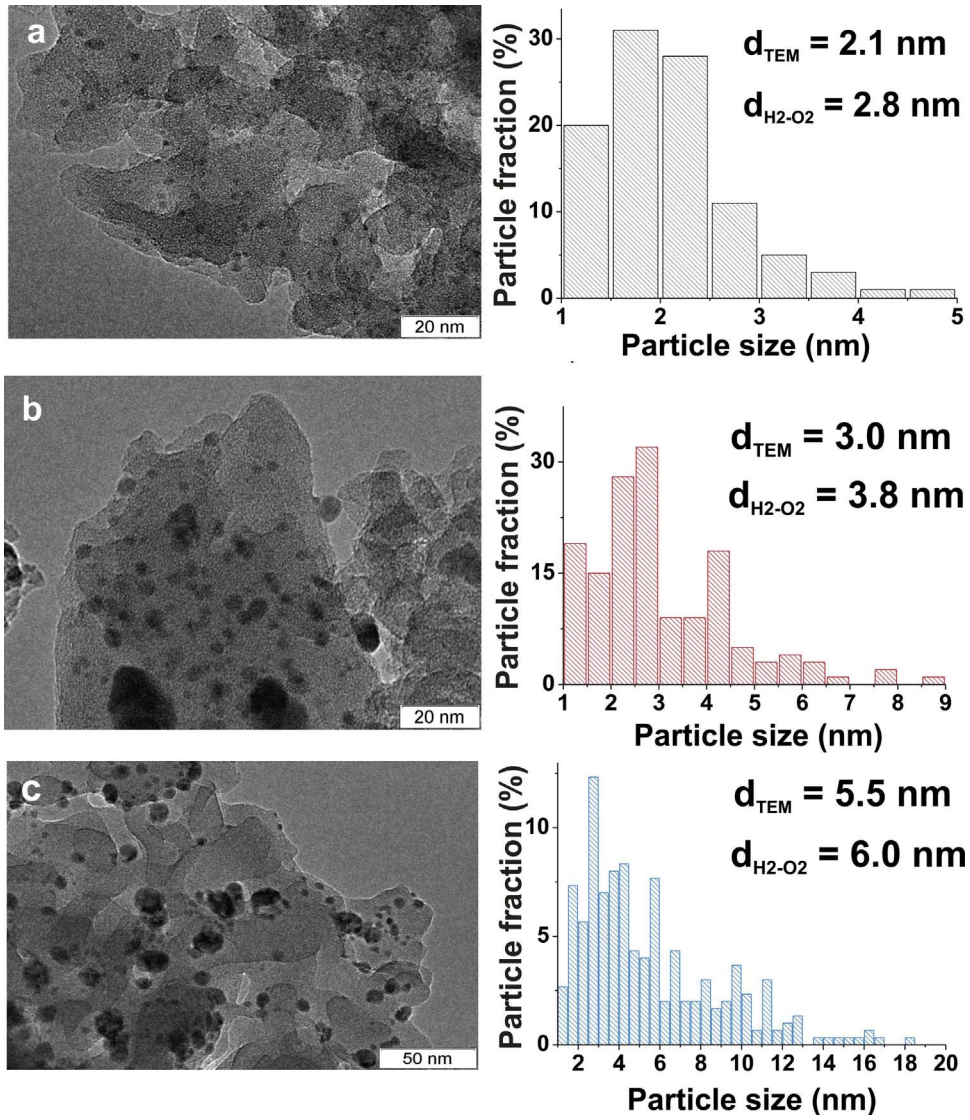

Fig. 5. TEM images (left) of 5Ag/SiO_2-500 (a), 5Ag/SiO_2-700 (b) and 5Ag/SiO_2-900 (c) catalysts and corresponding particle size distributions (right).

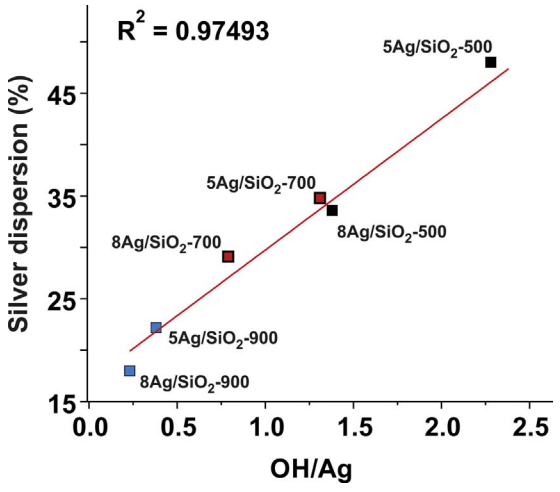

Fig. 6. Correlation between OH/Ag ratio and silver dispersion measured by H_2-O_2 titration method.

provides CO oxidation at RT because it does not retain CO_2.

Cao et al. investigated the oxidation of CO by silver clusters Ag_nO^- (n = 1-8). It was shown by DFT calculation that Ag_nO^- (n = 1, 2, 5–8) with terminal or bridging oxygen atoms generated free CO_2, and the quasi-linear structures of Ag_nO^- (n = 3, 4) generated chemically bonded CO_2 on silver [59]. Thus, theoretical investigations confirm the hypothesis about formation of two types of active sites on the silver surface with different ability to adsorb CO_2. We may conclude that double-peak activity in CO oxidation observed for some Ag/SiO_2 catalysts is associated with formation of carbonate species on the surface. The observed partial deactivation of the catalysts during CO oxidation at near-ambient temperatures is connected with blocking of active sites by adsorbed CO_2. When the temperature increases to up to 35 °C the carbonate species start to decompose and, hence, the activity grows up. However, the absence of double-activity peak for the 5Ag/SiO_2-500 catalyst is still not clear.

3.2.5. Investigation of reaction ability of adsorbed oxygen species

According to the literature data [33,36], the Ag/SiO_2 catalysts should be reduced in H_2 flow at 200–300 °C to achieve the highest catalytic activity in CO oxidation. However, the nature of active sites that participate in low-temperature CO oxidation is not discussed. Formation of subsurface oxygen is the prevalent point of view to explan the activity of Ag/SiO_2 composites [42,46]. Here we present new insights on the catalytic activity of Ag/SiO_2 catalysts.

To explore the reaction ability of adsorbed oxygen species TPR-H_2 and TPSR-CO experiments were carried out. Fig. 10 shows the TPR-H_2

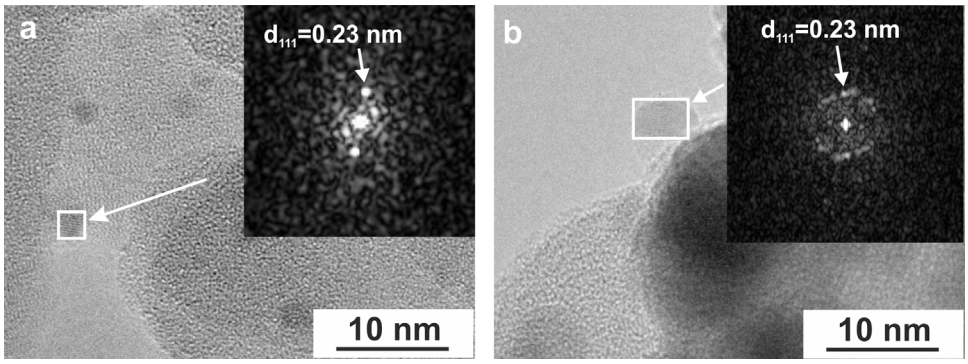

Fig. 7. TEM images and relevant Fourier patterns for 5Ag/SiO_2-500 and 5Ag/SiO_2-900 catalysts.

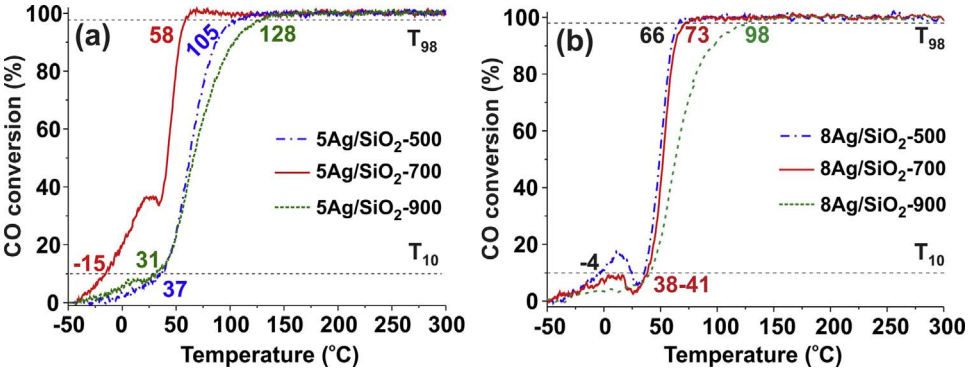

Fig. 8. Catalytic properties of 5Ag/SiO_2 (a) and 8Ag/SiO_2 (b) catalysts in CO oxidation after oxidative pretreatment at 500 °C followed by reduction at 200 °C.

profiles for the 5Ag/SiO_2 catalysts after oxidative pretreatment at 500 °C followed by reduction in H_2 at 200 °C, and adsorption of oxygen at 25 °C. TPR-H_2 data are reported in Table A1, Appendix A of Supplementary material. Two regions of hydrogen consumption can be marked. In the low-temperature region the intensive peaks with T_{max} = 83–100 °C are observed for all samples. Weak broad peaks in the range of 350–500 °C and 450–550 °C are observed in the high temperature region only for the 5Ag/SiO_2-500 and 5Ag/SiO_2-700 samples, respectively (see the inset). High temperature peaks are attributed to reduction of Si-O-Ag species [56] as mentioned above, while low-temperature peaks may be associated with reaction of adsorbed oxygen. It is noteworthy that the low-temperature peaks of H_2 consumption for the Ag/SiO_2-700 and Ag/SiO_2-900 samples consist of two overlapped peaks with similar value of T_{max}, however, only a single low-temperature peak was observed for Ag/SiO_2-500 sample. Thus, several types of adsorbed oxygen may exist on the surface of Ag/SiO_2-700 and Ag/SiO_2-900 catalysts. Total amount of oxygen atoms adsorbed at 25 °C was equal to 56, 51 and 33 μmol/g for the Ag/SiO_2-500, Ag/SiO_2-700 and Ag/SiO_2-900 catalysts, respectively.

Reaction ability of the active sites toward CO was investigated by means of TPSR-CO. Fig. 11 shows the CO_2 desorption profiles after adsorption of CO at −70 °C on the 5Ag/SiO_2 catalysts subjected to oxidative pretreatment at 500 °C followed by the reduction at 200 °C and re-adsorption of oxygen at 25 °C. Desorption peak of CO_2 in the range of ~40–180 °C is observed only for the 5Ag/SiO_2-700 and 5Ag/SiO_2-900 samples. The concentration of CO_2 desorbed from the surface of 5Ag/SiO_2-700 and 5Ag/SiO_2-900 catalysts and calculated from desorption peak area is ~21 and ~14 μmol/g, respectively. This means that the adsorption and oxidation of CO at −70 °C occurs with formation of adsorbed carbonate species only on the surface of 5Ag/SiO_2-700 and 5Ag/SiO_2-900 catalysts. Thus, the reaction ability of the adsorbed oxygen on the surfaces of 5Ag/SiO_2-500 and 5Ag/SiO_2-700, 5Ag/SiO_2-900 catalysts is different. Active sites on the surface of the 5Ag/SiO_2-700 and 5Ag/SiO_2-900 catalysts are much more reactive in comparison with those of the 5Ag/SiO_2-500. High reaction ability of the adsorbed oxygen may be associated with low strength of Ag_s-O_{ads} bond.

Fig. 12 shows the TPD-O_2 profiles for the 5Ag/SiO_2 catalysts after oxidative pretreatment followed by reduction at 200 °C and re-

Table 2
Comparison of catalytic activity in CO oxidation for different Ag/SiO_2 catalysts.

Catalyst	Ag, wt.%	Specific activity·10^{-6}, mol-CO/(m^2*h)[a]	TOF[b], h^{-1}	Reaction conditions				Ref.
				GHSV, ml/(g*h)	T, °C	X_{CO},%	CO/O_2	
Ag/SBA-15	8	6.2	5.0	9000	65	100	1/20	[39]
Ag/HMS	2.7	4.0	14.7	9000	100	100	1/20	[37]
Ag/SiO_2-500	8	30.0	6.5	12,000	66	98	1/1	[This work]
Ag/SiO_2-700	5	36.0	10.4	12,000	58	98	1/1	[This work]
Ag/HMS	2.8	3.6	15.2	9000	20	98	1/20	[17]
Ag/KIT-6	3.78	9.0	10.5	9000	90	100	1/20	[19]
Ag/SBA-15	8	6.1	4.9	9000	60	98	1/20	[24]
Ag/SBA-15	1.42	9.5	27.4	9000	20	98	1/20	[33]

[a] Catalytic activity calculated in accordance with value of specific surface area of the catalyst by Eq. A3 (See Appendix A of Supplementary material).
[b] Catalytic activity calculated as *mol-CO/(mol-Ag*h)* in accordance with total silver loading in the catalysts (different silver dispersion was ignored) by Eq. A4 (See Appendix A of Supplementary material).

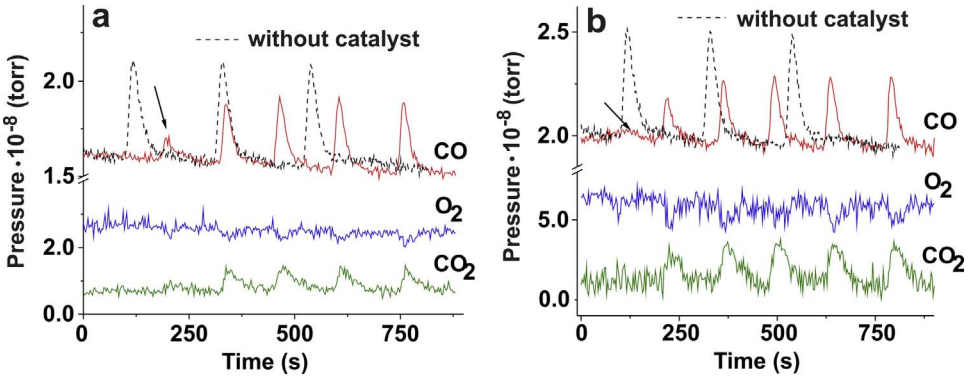

Fig. 9. Evolution of CO, O_2, and CO_2 concentration during pulse CO adsorption on the 5Ag/SiO_2-500 and 5Ag/SiO_2-700 catalysts at RT.

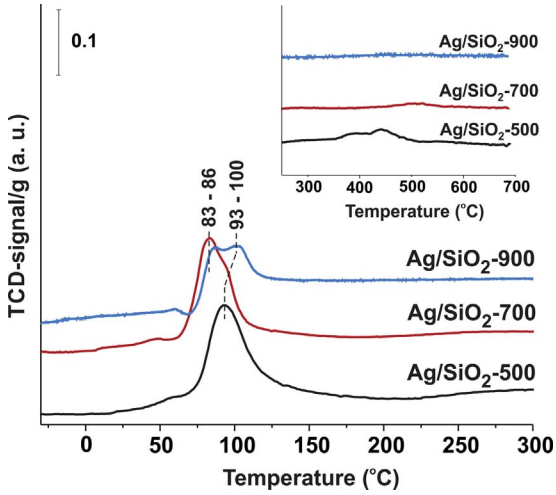

Fig. 10. TPR-H_2 profiles for 5Ag/SiO_2 catalysts after oxidative pretreatment followed by reduction in H_2 at 200 °C and adsorption of oxygen at 25 °C.

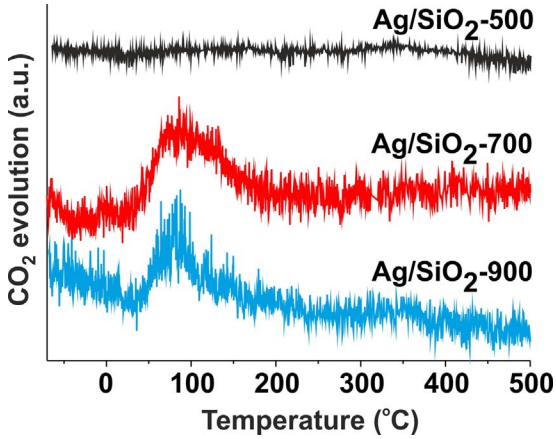

Fig. 11. TPSR-CO profiles (CO_2 desorption traces) for Ag/SiO_2 samples (5 wt.%) after adsorption of CO at −70 °C.

adsorption of oxygen at 25 °C. After deconvolution procedure, the peaks for three types of adsorbed oxygen are observed: two low-temperature species at ~390–420 and 490–560 °C, respectively, and a high temperature species at 670–740 °C. High temperature species is observed for all samples, however, the low-temperature peak at ~390–420 °C appears only for the Ag/SiO_2-700 and Ag/SiO_2-900 samples. Moreover, the amount of another low-temperature species is higher for the Ag/SiO_2-700 and Ag/SiO_2-900 samples in comparison with those of Ag/SiO_2-500. These low-temperature species provide high activity of Ag/SiO_2-700 and Ag/SiO_2-900 in CO oxidation.

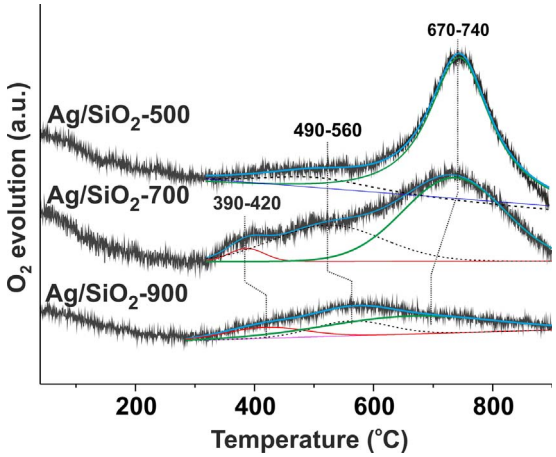

Fig. 12. TPD-O_2 profiles for 5Ag/SiO_2 catalysts after oxidative pretreatment at 500 °C followed by reduction at 200 °C and re-adsorption of oxygen at 25 °C.

3.2.6. *Tentative scheme of CO oxidation at RT*

The changing of oxygen desorption temperature may be associated with different nature of Ag_s—O_{ads} bonds. Low-temperature species at 390–420 °C is similar to oxygen of bulk Ag_2O with the same desorption temperature, whereas the nature of the high-temperature form is different. Adsorption of several oxygen species for Ag/SiO_2-700 and Ag/SiO_2-900 catalysts may be associated with multidomain structure of Ag NPs that was shown early for the Ag/SiO_2-900 catalyst in [58]. Adsorption of weakly bound oxide-like oxygen species with high reaction ability toward CO on the surface of the Ag/SiO_2-700 and Ag/SiO_2-900 samples probably occurs with participation of the extended intergrain boundaries of defective Ag NPs. As known, oxygen of Ag_2O is strongly ionic by its nature, and Ag-O bond is polarized [60]. Adsorption of strongly ionic oxygen with E_b (O1s) < 529 eV over silver NPs having defective structure prepared by thermal evaporation of silver and sputtering of the silver electrode by radio-frequency discharge in oxygen-containing atmosphere was mentioned in [45]. Existence of two different types of oxygen on the silver surface was described in [49,61–63]. The first type is so called “nucleophilic” (ionic) oxygen with effective charge of 1.65 *e*, and the second type is “electrophilic” (covalent) oxygen with effective charge of 0.35 *e* [64,65]. When nucleophilic oxygen adsorbs on the silver surface, the additional delocalization of electron density with formation of Lewis Ag^+ sites occurs [49]. The Ag^+ sites may be favorable for adsorption and activation of CO molecules.

Weakly bound oxygen species possess the high reaction ability toward CO that was confirmed by TPSR-CO. From this point of view, appearance of double-peak activity for 5Ag/SiO_2-700 and 5Ag/SiO_2-900 catalysts in catalytic experiments may be associated with high rate of CO oxidation at subambient temperatures (from −50 to 10 °C) and accumulation of adsorbed carbonates on the surface. Adsorption of

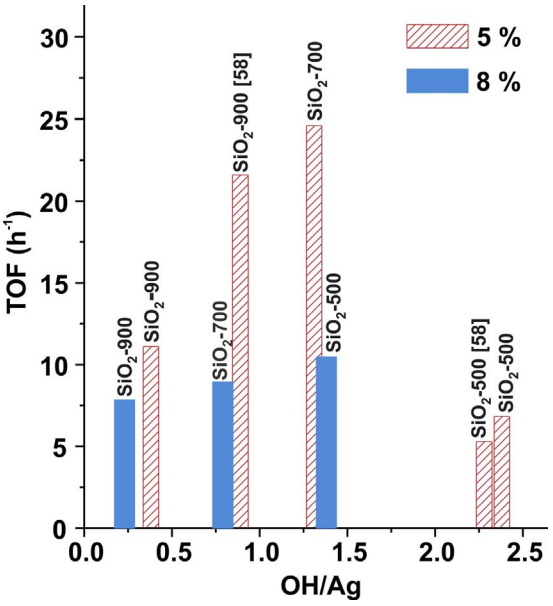

Fig. 13. Dependence of TOFs from ratio OH/Ag for different Ag/SiO_2 catalysts prepared in this work and in [58].

CO_2 on active sites leads to gradual decreasing of catalytic activity. Increase of reaction temperature leads to decomposition of adsorbed carbonate species and growth of CO conversion. Absence of active sites with high reaction ability on the surface of $5Ag/SiO_2$-500 leads to low rate of CO oxidation at subambient temperatures, and hence, no visible deactivation is observed. In other words, reaction of CO oxidation starts at higher temperatures for $5Ag/SiO_2$-500 in comparison with $5Ag/SiO_2$-700 and $5Ag/SiO_2$-900 catalysts. However, for $8Ag/SiO_2$-500 catalyst a considerable amount of weakly bound oxygen species appears due to formation of defective Ag NPs (See Fig. A6, Appendix A of Supplementary material), and hence, double-peak activity in CO oxidation is observed for $8Ag/SiO_2$-500. Thus, all catalysts with low OH/Ag ratio are characterized by the presence of highly reactive oxygen species and double-peak activity in CO oxidation.

Fig. 13 shows the correlation between the OH/Ag ratio and TOFs (calculated per amount of surface silver atoms according to H_2—O_2 titration data) at 50 °C for the Ag/SiO_2 catalysts prepared in this work and in [58]. One can see the volcano-shape dependency of TOF values on OH/Ag ratio for the $5Ag/SiO_2$, which is caused by simultaneous changing of dispersion and structure of the Ag NPs. Formation of silver NPs possessing high dispersion and monodomain structure occurs at OH/Ag ratios above 2. These NPs are not so highly active in CO oxidation. Formation of defective Ag NPs having relatively high dispersion occurs at optimal OH/Ag ratio (~0.8–1.5). These NPs possess high activity due to weakly bound oxygen species adsorbed on the surface. Dispersion of silver nanoparticles decreases significantly at OH/Ag ratios below 0.5, and hence, the activity in CO oxidation drops. Thus, high activity in CO oxidation may be achieved only at optimal value of the OH/Ag ratio. However, the activity of Ag/SiO_2 catalysts, containing 8 wt.% of silver, grows up slowly with increasing of the OH/Ag ratio. We deduced that the properties of the support influence on the catalytic activity in a lesser extent for the Ag/SiO_2 catalysts with a high silver loading. The TOF values for the $8Ag/SiO_2$ samples are lower in comparison with those for the $5Ag/SiO_2$ except for the catalysts prepared on the basis of SiO_2-500 support. There are two reasons for this phenomenon. Firstly, the amount of active sites decreases due to lowering of silver dispersion with an increase of silver content. Secondly, the reaction rate (TOFs) are normalized on the higher amount of silver atoms.

In this paper, we assume the nature of different active sites on the surface of Ag/SiO_2 catalysts. Fig. 14 shows the tentative scheme of CO oxidation at RT on the Ag/SiO_2 catalysts with different OH/Ag ratio. Oxygen species adsorbed on the silver NPs near the silica–silver interface (marked with black color on the image) have lower effective charge in comparison with other species due to delocalization of electron density caused by metal–support interaction. Formation of $Ag^{\delta+}$ sites even after reduction of Ag/SiO_2 catalysts at 500 °C in H_2 was confirmed by FTIR of adsorbed CO [42]. Basicity of adsorbed oxygen species depends on their effective charge. Decreasing of oxygen effective charge leads to lowering of basicity. As a consequence, CO_2 formed after interaction of CO molecule with this type of adsorbed oxygen species desorbs easily at RT. Another type of oxygen (marked with blue color in the image) has higher effective charge and may adsorb weakly bound carbonate species (probably, monodentate species) that decomposes above room temperature. For defective Ag NPs an adsorption of additional form of weakly bound oxygen species (marked with white color in the image) occurs at the extended intergrain boundaries. These species have high reaction ability and, as a consequence, react with CO even at subambient temperatures.

Briefly, silver NPs with appropriate dispersion and defective structure may adsorb weakly bound oxygen species which are responsible for high catalytic activity in CO oxidation. The OH/Ag ratio plays a crucial role in designing of highly effective Ag/SiO_2 catalysts.

4. Conclusion

The Ag/SiO_2 catalysts (5 and 8 wt.%) prepared on the basis of silica calcined at 500, 700 and 900 °C were investigated. Active surfaces of the catalysts were characterized in details. For the first time, the OH/Ag ratio (molar ratio between the concentration of surface SiOH groups normalized to support mass and silver amount in the prepared catalysts) has been proposed for Ag/SiO_2 catalysts as a crucial factor to achieve high activity in CO oxidation. Formation of Ag nanoparticles with different dispersion and structure is observed after oxidative pretreatment (500 °C) followed by reduction of the catalysts by H_2/Ar at 200 °C. The dispersion of silver NPs decreases with lowering of OH/Ag ratio. Moreover, silver NPs in the catalysts with low OH/Ag ratio possess the defective structure (consisted of several crystal nanodomains).

Two types of active sites with respect to CO_2 adsorption ability are shown to exist on the surface of Ag/SiO_2 catalysts. The first type of active sites is catalytically active at room temperature because it does not adsorb CO_2. The second type may retain surface carbonate species that start decomposing only at ~40–50 °C.

The OH/Ag ratio influences on the redispersing of silver particles under repeated oxidative pretreatment at 500 °C. Full redispersing and oxidation of silver nanoparticles with formation of AgO_x species is observed for the catalyst with OH/Ag ratio above 2. At the same time, only partial redispersing and oxidation of Ag nanoparticles occurs in the case of the lower OH/Ag ratio (< 1.5).

Silver nanoparticles are shown to be able to adsorb several oxygen species at RT with different strength of Ag—O bond. The presence of weakly bound oxygen species with high reaction ability toward CO (even at −70 °C) is observed for the Ag/SiO_2 catalysts with low OH/Ag ratio. These species are probably adsorbed on the extended intergrain boundaries of defective Ag nanoparticles. Weakly bound oxygen species provid high activity in CO oxidation at low temperatures. However, the dispersion of Ag nanoparticles as well as weakly bound oxygen species play a crucial role. Only at optimal value of OH/Ag ratio (0.8–1.5) the defective Ag NPs with relatively high dispersion (d = 3-5 nm) and, hence, high concentration of active oxygen species, may be obtained. When silver dispersion diminished significantly with decreasing of the OH/Ag ratio, the catalytic activity drops (OH/Ag $<$ 0.5). On the other hand, silver NPs with sizes 1–3 nm (high dispersion) formed at OH/Ag $>$ 2 do not adsorb weakly bound oxygen, hence, the activity of the catalysts is not high. The dependency of turnover frequency (TOF) for the Ag/SiO_2 catalysts on the OH/Ag ratio is a volcano-shape one due to simultaneous changing of dispersion and structure of the Ag NPs. Thus, high activity in CO oxidation may be achieved at optimal value of the

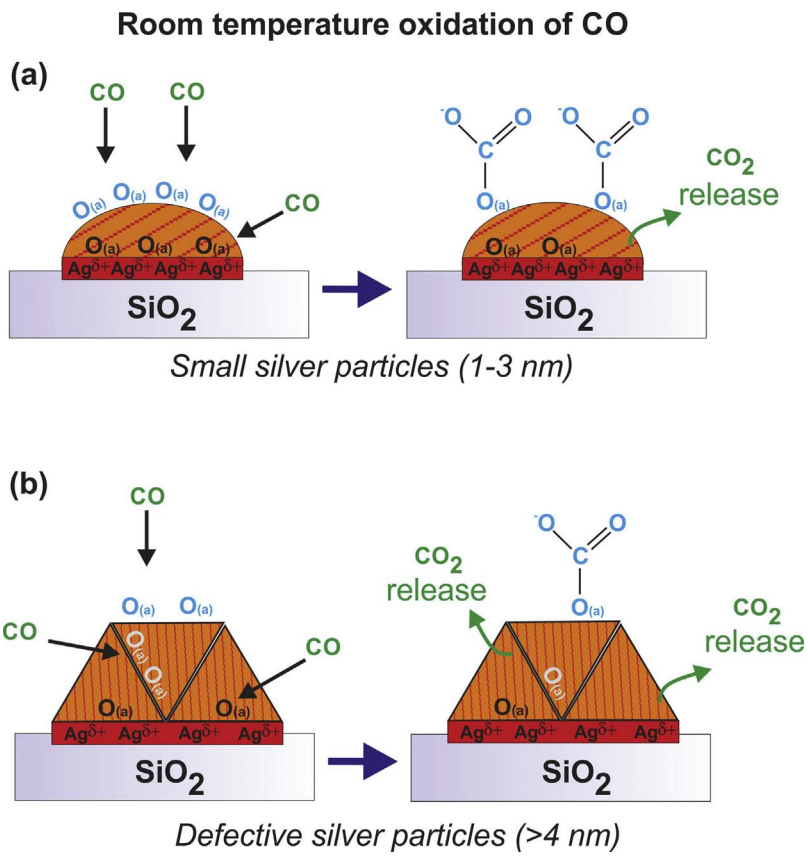

Fig. 14. Tentative scheme of CO oxidation at RT on the Ag NPs with different dispersion and structure.

OH/Ag ratio.

Acknowledgment

This work was supported by the Tomsk State University Competitiveness Improvement Program (8.2.19.2017). This work was carried out also as part of a government task of the Russian Ministry of Education and Science (project no. 4.4590.2017/6.7). The authors thank Dr. Michael Salaev (Tomsk State University) for language review.

Appendix A. Supplementary data

Supplementary data associated with this article can be found, in the online version, at http://dx.doi.org/10.1016/j.apcatb.2017.09.051.

References

[1] T. Biemelt, K. Wegner, J. Teichert, M.R. Lohe, J. Martin, J. Grothe, S. Kaskel, Hopcalite nanoparticle catalysts with high water vapor stability for catalytic oxidation of carbon monoxide, Appl. Catal. B: Environ. 184 (2016) 208–215.
[2] M.J. Kale, D. Gidcumb, F.J. Gulian, S.P. Miller, C.H. Clark, P. Christopher, Evaluation of platinum catalysts for naval submarine pollution control, Appl. Catal. B: Environ. 203 (2017) 533–540.
[3] C. Qi, H. Su, R. Guan, H. Lin, X. Sun, Y. Zheng, Application of alumina-based nanogold catalysts in CO_2 laser, Technical Proceedings of the 2014 NSTI Nanotechnology Conference and Expo, NSTI-Nanotech 2014 3 (2014) 296–299.
[4] S. Arunkumar, T. Hou, Y.-B. Kim, B. Choi, S.H. Park, S. Jung, D.-W. Lee, Au Decorated ZnO hierarchical architectures: facile synthesis, tunable morphology and enhanced CO detection at room temperature, Sens. Actuators B 243 (2017) 990–1001.
[5] L. Pahalagedara, D.A. Kriz, N. Wasalathanthri, C. Weerakkody, Y. Meng, S. Dissanayake, M. Pahalagedara, Z. Luo, S.L. Suib, P. Nandid, R.J. Meyer, Benchmarking of manganese oxide materials with CO oxidation as catalysts for low temperature selective oxidation, Appl. Catal. B: Environ. 204 (2017) 411–420.
[6] A.A. Vedyagin, A.M. Volodin, R.M. Kenzhin, V.V. Chesnokov, Ilya V. Mishakov, CO oxidation over Pd/ZrO_2 catalysts: role of supports donor sites, Molecules 1 (10) (2016) 1289–1303.
[7] D. Gu, J.-C. Tseng, C. Weidenthaler, H.-J. Bongard, B. Spliethoff, W. Schmidt, F. 7Soulimani, B.M. Weckhuysen, F. Schuth, Gold on different manganese oxides: ultra-low-temperature CO oxidation over colloidal gold supported on Bulk-MnO_2 nanomaterials, J. Am. Chem. Soc. 138 (30) (2016) 9572–9580.
[8] C. Wang, C. Wen, J. Lauterbach, E. Sasmaz, Superior oxygen transfer ability of Pd/MnO_x-CeO_2 for enhanced low temperature CO oxidation activity, Appl. Catal. B: Environ. 206 (2017) 1–8.
[9] K. Yang, Y. Zhang, Y. Li, P. Huang, X. Chen, W. Dai, X. Fu, Insight into the function of alkaline earth metal oxides as electron promoters for Au/TiO_2 catalysts used in CO oxidation, Appl. Catal. B: Environ. 183 (2016) 206–215.
[10] O.H. Laguna, A. Perez, M.A. Centeno, J.A. Odriozola, Synergy between gold and oxygen vacancies in gold supported on Zr-doped ceria catalysts for the CO oxidation, Appl. Catal. B: Environ. 176–177 (2015) 385–395.
[11] E.M. Slavinskaya, R.V. Gulyaev, A.V. Zadesenets, O.A. Stonkus, V.I. Zaikovskii, Yu V. Shubin, S.V. Korenev, A.I. Boronin, Low-temperature CO oxidation by Pd/CeO_2 catalysts synthesized using the co-precipitation method, Appl. Catal. B: Environ. 166–167 (2015) 91–103.
[12] Z. Qu, S. Shen, D. Chen, Y. Wang, Highly active Ag/SBA-15 catalyst using post-grafting method for formaldehyde oxidation, J. Mol. Catal. A: Chem. 356 (2012) 171–177.
[13] D. Chen, Z. Qu, Y. Sun, K. Gao, Y. Wang, Identification of reaction intermediates and mechanism responsible for highly active HCHO oxidation on Ag/MCM-41 catalysts, Appl. Catal. B: Environ. 142–143 (2013) 838–848.
[14] D. Chen, Z. Qu, Y. Lv, X. Lu, W. Chen, X. Gao, Effect of oxygen pretreatment on the surface catalytic oxidation of HCHO on Ag/MCM-41 catalysts, J. Mol. Catal. A: Chem. 404–405 (2015) 98–105.
[15] D. Chen, Z. Qu, S. Shen, X. Li, Y. Shi, Y. Wang, Q. Fu, J. Wu, Comparative studies of silver based catalysts supported on different supports for the oxidation of formaldehyde, Catal. Today 175 (2011) 338–345.
[16] Z. Qu, Y. Bu, Y. Qin, Y. Wang, Q. Fu, The improved reactivity of manganese catalysts by Ag in catalytic oxidation of toluene, Appl. Catal. B: Environ. 132–133 (2013) 353–362.
[17] Z. Qu, X. Zhang, F. Yu, J. Jia, A simple one pot synthesis of mesoporous silica hosted silver catalyst and its low-temperature CO oxidation, Microporous Mesoporous Mater. 188 (2014) 1–7.
[18] H. Liu, D. Ma, R.A. Blackley, W. Zhou, X. Bao, Highly active mesostructured silica hosted silver catalysts for CO oxidation using the one-pot synthesis approach, Chem. Commun. 23 (2008) 2677–2679.
[19] Y. Yang, F. Hou, H. Li, N. Liu, Y. Wang, X. Zhang, Facile synthesis of Ag/KIT-6 catalyst via a simple one pot method and application in the CO oxidation, J. Porous Mater. (2017), http://dx.doi.org/10.1007/s10934-017-0406-1.
[20] Z.P. Qu, X.D. Zhang, F.L. Yu, X.C. Liu, Q. Fu, Role of the Al chemical environment in the formation of silver species and its CO oxidation activity, J. Catal. 321 (2015) 113–122.
[21] Z. Qu, M. Cheng, C. Shi, X. Bao, Low-temperature selective oxidation of CO in H_2-rich gases over Ag/SiO_2 catalysts, J. Mol. Catal. A: Chem. 239 (2005) 22–31.

[22] L. Li, Z. Yang, Y. Yuan, Y. Zhang, J. Li, Synthesis and characterization of nanosilver catalysts supported on the nitrogen-incorporated-SBA-15 for the low-temperature selective CO oxidation, J. Porous Mater. 22 (2015) 1473–1482.
[23] X.D. Zhang, H. Dong, Z.J. Gu, G. Wang, Y.H. Zuo, Y.G. Wang, L.F. Cui, Preferential carbon monoxide oxidation on Ag/Al-SBA-15 catalysts: effect of the Si/Al ratio, Chem. Eng. J. 269 (2015) 94–104.
[24] X. Zhang, H. Dong, Y. Wang, N. Liu, Y. Zuo, L. Cui, Study of catalytic activity at the Ag/Al-SBA-15 catalysts for CO oxidation and selective CO oxidation, Chem. Eng. J. 283 (2016) 1097–1107.
[25] T. Kharlamova, G. Mamontov, M. Salaev, V. Zaikovskii, G. Popova, V. Sobolev, A. Knyazev, O. Vodyankina, Silica-supported silver catalysts modified by cerium/manganese oxides for total oxidation of formaldehyde, Appl. Catal. A: Gen. 467 (2013) 519–529.
[26] G.V. Mamontov, V.V. Dutov, V.I. Sobolev, O.V. Vodyankina, Effect of transition metal oxide additives on the activity of an Ag/SiO_2 catalyst in carbon monoxide oxidation, Kinet. Catal. 54 (4) (2013) 487–491.
[27] G.V. Mamontov, M.V. Grabchenko, V.I. Sobolev, V.I. Zaikovskii, O.V. Vodyankina, Ethanol dehydrogenation over $Ag\text{-}CeO_2/SiO_2$ catalyst: role of $Ag\text{-}CeO_2$ interface, Appl. Catal. A: Gen. 528 (2016) 161–167.
[28] V.L. Sushkevich, I.I. Ivanova, E. Taarning, Mechanistic study of ethanol dehydrogenation over silica-Supported silver, ChemCatChem 5 (2013) 2367–2373.
[29] V.V. Dutov, G.V. Mamontov, V.I. Sobolev, O.V. Vodyankina, Silica-supported silver-containing OMS-2 catalysts for ethanol oxidative dehydrogenation, Catal. Today 278 (2016) 164–173.
[30] L. Ma, J.X. ia, L. Xiang, Catalytic activity of Ag/SBA-15 for low-temperature gas--phase selective oxidation of benzyl alcohol to benzaldehyde, Chin. J. Catal. 35 (2014) 108–119.
[31] V.K. Tomer, S. Duhan, R. Malik, S.P. Nehra, Fast response with high performance humidity sensing of $Ag\text{-}SnO_2$/SBA-15 nanohybrid sensors, Microporous Mesoporous Mater. 219 (2016) 240–248.
[32] J.E. Lee, S. Bera, Y.S. Choi, W.I. Lee, Size-dependent plasmonic effects of M and M@SiO_2 (M = Au or Ag) deposited on TiO_2 in photocatalytic oxidation reactions, Appl. Catal. B: Environ. 214 (2017) 15–22.
[33] X. Zhang, Z. Qu, F. Yu, Y. Wang, High-temperature diffusion induced high activity of SBA-15 supported Ag particles for low temperature CO oxidation at room temperature, J. Catal. 297 (2013) 264–271.
[34] D. Afanasev, O. Yakovina, N. Kuznetsova, A. Lisitsyn, High activity in CO oxidation of Ag nanoparticles supported on fumed silica, Catal. Comm. 22 (2012) 43–47.
[35] X.D. Zhang, Z.P. Qu, F.L. Yu, Y. Wang, Progress in carbon monoxide oxidation over nanosized Ag catalysts, Chin. J. Catal. 34 (2013) 1277–1290.
[36] X. Zhang, Z. Qu, X. Li, M. Wen, X. Quan, D. Ma, J. Wu, Studies of silver species for low-temperature CO oxidation on Ag/SiO_2 catalysts, Sep. Purif. Technol. 72 (2010) 395–400.
[37] X. Zhang, Z. Qu, J. Jia, Y. Wang, Ag nanoparticles supported on wormhole HMS material as catalysts for CO oxidation: effects of preparation methods, Powder Technol. 230 (2012) 212–218.
[38] X. Zhang, Z. Qu, X. Li, Q. Zhao, Y. Wang, X. Quan, Low temperature CO oxidation over Ag/SBA-15 nanocomposites prepared via in-situ pH-adjusting method, Catal. Commun. 16 (2011) 11–14.
[39] X. Zhang, Z. Qu, F. Yu, Y. Wang, X. Zhang, Effects of pretreatment atmosphere and silver loading on the structure and catalytic activity of Ag/SBA-15 catalysts, J. Mol. Catal. A: Chem. 370 (2013) 160–166.
[40] Z. Qu, W. Huang, S. Zhou, H. Zheng, X. Liu, M. Cheng, X. Bao, Enhancement of the catalytic performance of supported-metal catalysts by pretreatment of the support, J. Catal. 234 (2005) 33–36.
[41] X.D. Zhang, H. Dong, D. Zhao, Y. Wang, Y.G. Wang, L.F. Cui, Effect of support calcination temperature on Ag structure and catalytic activity for CO oxidation, Chem. Res. Chin. Univ. 32 (2016) 455–460.
[42] Z. Qu, M. Cheng, W. Huang, X. Bao, Formation of subsurface oxygen species and its high activity toward CO oxidation over silver catalysts, J. Catal. 229 (2005) 446–458.
[43] L. Yu, Y. Shi, Z. Zhao, H. Yin, Y. Wei, J. Liu, W. Kang, Ultrasmall silver nanoparticles supported on silica and their catalytic performances for carbon monoxide oxidation, Catal. Commun. 12 (2011) 616–620.
[44] N. Turaeva, M.L. Preuss, Electronic effects in CO oxidation by nanoparticle catalysts, Catal. Commun. 65 (2015) 30–33.
[45] L.S. Kibis, A.I. Stadnichenko, E.M. Pajetnov, S.V. Koscheeva, V.I. Zaykovskii, A.I. Boronin, The investigation of oxidized silver nanoparticles prepared by thermal evaporation and radio-frequency sputtering of metallic silver under oxygen, Appl. Surf. Sci. 257 (2010) 404–413.
[46] Z. Qu, W. Huang, M. Cheng, X. Bao, Restructuring and redispersion of silver on SiO_2 under oxidizing/reducing atmospheres and its activity toward CO oxidation, J. Phys. Chem. B 109 (2005) 15842–15848.
[47] L.T. Zhuravlev, The surface chemistry of amorphous silica. Zhuravlev model, Coll. Surf. A: Physicochem. Eng. Asp. 173 (2000) 1–38.
[48] L. Zhang, C. Zhang, H. He, The role of silver species on Ag/Al_2O_3 catalysts for the selective catalytic oxidation of ammonia to nitrogen, J. Catal. 261 (2009) 101–109.
[49] V.I. Bukhtiyarov, A.I. Boronin, V.I. Savchenko, Stages in the modification of a silver surface for catalysis of the partial oxidation of ethylene, J. Catal. 150 (1994) 262–267.
[50] S.R. Seyedmonir, D.E. Strohmayer, G.L. Geoffroy, M.A. Vannice, Characterization of supported silver catalysts, J. Catal. 87 (1984) 424–436.
[51] D.E. Strohmayer, G.L. Geoffroy, M.A. Vannice, Measurement of silver surface area by the H_2 titration of chemisorbed oxygen, Appl. Catal. 7 (1983) 189–198.
[52] S. Pal, Y.K. Tak, J.M. Song, Does the antibacterial activity of silver nanoparticles depend on the shape of the nanoparticle? a study of the gram-Negative bacterium *Escherichia coli*, Appl. Environ. Microbiol. 73 (2007) 1712–1720.
[53] R. Brause, H. Möltgen, K. Kleinermanns, Characterization of laser-ablated and chemically reduced silver colloids in aqueous solution by UV/VIS spectroscopy and STM/SEM microscopy, Appl. Phys. B 75 (2002) 711–716.
[54] H. Bi, W. Cai, L. Zhang, D. Martin, F. Träger, Annealing-induced reversible change in optical absorption of Ag nanoparticles, Appl. Phys. Lett. 81 (2002) 5222–5224.
[55] Z. Qu, M. Cheng, X. Dong, X. Bao, CO selective oxidation in H_2-rich gas over Ag nanoparticles – effect of oxygen treatment temperature on the activity of silver particles mechanically mixed with SiO_2, Catal. Today 93–95 (2004) 247–255.
[56] G.V. Mamontov, T.I. Izaak, O.V. Magaev, A.S. Knyazev, O.V. Vodyankina, Reversible oxidation/reduction of silver supported on silica aerogel: influence of the addition of phosphate, Rus. J. Phys. Chem. A 85 (9) (2011) 1540–1545.
[57] M. Kosmulski, Isoelectric points and points of zero charge of metal (hydr)oxides: 50 years after Parks' review, Adv. Colloid Interface Sci. 238 (2016) 1–61.
[58] V.V. Dutov, G.V. Mamontov, V.I. Zaikovskii, O.V. Vodyankina, The effect of support pretreatment on activity of Ag/SiO_2 catalysts in low-temperature CO oxidation, Catal. Today 278 (2016) 150–156.
[59] X. Cao, M. Chen, J. Ma, B. Yin, X. Xing, CO oxidation by the atomic oxygen on silver clusters: structurally dependent mechanisms generating free or chemically bonded CO_2, Phys. Chem. Chem. Phys. 19 (2017) 196–203.
[60] A.I. Boronin, S.V. Koscheev, G.M. Zhidomirov, XPS and UPS study of oxygen states on silver, J. Electron Spectrosc. Relat. Phenom. 96 (1998) 43–51.
[61] V.I. Bukhtiyarov, V.V. Kaichev, The combined application of XPS and TPD to study of oxygen adsorption on graphite-supported silver clusters, J. Mol Catal. A: Chem. 158 (2000) 167–172.
[62] V.I. Bukhtiyarov, A.I. Boronin, V.I. Savchenko, Two oxygen states and the role of carbon in partial oxidation of ethylene over silver, Surf. Sci. Lett. 232 (1990) 205–209.
[63] V.I. Bukhtiyarov, A.F. Carley, L.A. Dollard, M.W. Roberts, XPS study of oxygen adsorption on supported silver: effect of particle size, Surf. Sci. 381 (1997) 605–608.
[64] V.V. Kaichev, V.I. Bukhtiyarov, M. Havecker, A. Knop-Gercke, R.W. Mayer, R. Schlögl, The nature of electrophilic and nucleophilic oxygen adsorbed on silver, Kinet. Catal. 44 (2003) 432–440.
[65] V.I. Bukhtiyarov, M. Havecker, V.V. Kaichev, A. Knop-Gericke, R.W. Mayer, R. Schlögl, Atomic oxygen species on silver: photoelectron spectroscopy and X-ray absorption studies, Phys. Rev. B 67 (2003) 2354221–23542212.